High-pressure synthesis and exotic heavy-fermion behaviour of the filled skutterudite $SmPt_4Ge_{12}$

2010 New J. Phys. 12 103035

(http://iopscience.iop.org/1367-2630/12/10/103035)

New Journal of Physics
The open-access journal for physics

High-pressure synthesis and exotic heavy-fermion behaviour of the filled skutterudite $SmPt_4Ge_{12}$

R Gumeniuk[1], **M Schöneich**[2], **A Leithe-Jasper**[1], **W Schnelle**[1,3], **M Nicklas**[1], **H Rosner**[1], **A Ormeci**[1], **U Burkhardt**[1], **M Schmidt**[1], **U Schwarz**[1], **M Ruck**[2] **and Yu Grin**[1]

[1] Max-Planck-Institut für Chemische Physik fester Stoffe, Nöthnitzer Straße 40, 01187 Dresden, Germany
[2] Anorganische Chemie, Technische Universität Dresden, 01062 Dresden, Germany
E-mail: schnelle@cpfs.mpg.de

New Journal of Physics **12** (2010) 103035 (16pp)
Received 10 August 2010
Published 19 October 2010
Online at http://www.njp.org/
doi:10.1088/1367-2630/12/10/103035

Abstract. Ternary samarium-filled platinum–germanium skutterudite $SmPt_4Ge_{12}$ was prepared at a pressure of 5.0(0.5) GPa and a temperature of 1070(70) K. The compound crystallizes in the cubic space group $Im\bar{3}$ ($a = 8.6069(4)$ Å) and is isotypic with $LaFe_4P_{12}$. X-ray absorption spectroscopy measurements show that samarium in $SmPt_4Ge_{12}$ has a temperature-independent intermediate valence ($\nu = 2.90 \pm 0.03$). Magnetization data reveal Van Vleck paramagnetism above ∼50 K. The low-temperature specific heat displays a broad anomaly centred at 2.9 K and a large linear coefficient $\gamma' = 450\,\mathrm{mJ\,mol^{-1}\,K^{-2}}$ suggesting heavy-fermion behaviour. Low-temperature electrical resistivity shows a temperature dependence reminiscent of the Kondo effect. Density functional calculations result in an electronic structure that is, apart from the Sm $4f$ contributions, very similar to $LaPt_4Ge_{12}$.

---

[3] Author to whom any correspondence should be addressed.

Contents

1. Introduction

Filled skutterudites have become a topic of considerable interest with respect to basic and applied solid state sciences. This is mainly due to a variety of physical properties that are intimately related to the underlying structural chemistry [1]–[4]. Filled skutterudites have the general chemical formula $M_{1-x}T_4X_{12}$, with M representing an electropositive element such as an alkali, alkaline-earth, early rare-earth or actinide metal or the metal thallium, T representing a transition metal of the iron or cobalt group and X representing a pnictogen element such as phosphorus, arsenic or antimony. These compounds all crystallize with the cubic $LaFe_4P_{12}$ [5] structure.

In a simplified, qualitative picture of the chemical bonding, the filler metal atoms (with relatively low electronegativity) form cations and transfer valence electrons to a transition-metal pnictogen network. In the resulting polyanions $[T_4X_{12}]$, the transition metal centres the octahedra formed by a pnictogen. The spatial arrangement of these octahedra in the unit cell gives rise to the formation of large empty icosahedral spaces in the framework structure, which are occupied by the filler atoms. It has been shown that in most of the filled skutterudites, there exist certain size limitations for the filler atoms. This is most obvious for the rare-earth metal cations, which are restricted to the early members [6]. Also, it has been found difficult to obtain full occupancy on the icosahedral site with trivalent ions or with barium. A suitable tool for fine-tuning of the electron count and, thus, physical properties, is substitution of the constituting elements. Whereas early work concentrated on variations of the electropositive filler metal, later studies demonstrated the effects of partly substituting the host structure forming atoms by elements of the neighbouring groups in the periodic table [3].

Recently, it has been shown that the transition metal is not restricted to the iron or cobalt group but can also be the noble metal platinum, which together with germanium acts as the framework forming elements stabilized by the alkaline-earth metals Sr and Ba [7, 8]. Moreover, we have discovered a new family of rare-earth metal (R)-based filled skutterudites $R\mathrm{Pt_4Ge_{12}}$ with $R = \mathrm{La}$–Nd, and Eu [8, 9]. The lanthanum and praseodymium compounds are superconducting metals with $T_\mathrm{c} = 8.3$ and 7.9 K, whereas Sr and $\mathrm{BaPt_4Ge_{12}}$ have $T_\mathrm{c} \approx 5\,\mathrm{K}$ [8]. The isostructural compounds with trivalent Nd and divalent Eu are paramagnetic metals that order antiferromagnetically at 0.67 and 1.7 K, respectively, whereas in $\mathrm{CePt_4Ge_{12}}$ the Ce ions are intermediate-valent and do not order [8, 10, 11]. Meanwhile, further skutterudite compounds with $[\mathrm{Pt_4Ge_{12}}]$ host structure and actinoid cations have been synthesized ($A = \mathrm{Th}$, U [12, 13]).

Since some threshold size requirements exist for the filler atoms in order to stabilize a skutterudite, several studies have been devoted to probing high-pressure synthesis routes to compounds that are based on cations with radii below the critical value. This approach has been particularly successful with regard to rare-earth metals. Here, experiments have already revealed that ions with smaller radii than neodymium (i.e. $\mathrm{Sm^{3+}}$, $\mathrm{Gd^{3+}}$–$\mathrm{Tb^{3+}}$ and $\mathrm{Y^{3+}}$ for $T = \mathrm{Fe}$; La–Tb and Y for $T = \mathrm{Ru}$; and La–Ho and Y for $T = \mathrm{Os}$) can be inserted into a phosphorus-based framework in compounds $RT_4\mathrm{P}_{12}$ upon compression [14]–[18]. The currently known filled skutterudites with arsenic and antimony—which feature larger frameworks—accommodate rare-earth fillers La–Sm only (besides of course the larger divalent Eu and Yb ions).

On the other hand in tetrel chemistry, high-pressure preparations have enabled the preparation of new cage compounds—clathrates or penta- and hexatetrelides of the rare-earth metals [19]–[22]. For exhaustive reviews on skutterudite physics and chemistry, please refer to [3, 6, 23, 24].

Here, we report on the preparation, crystal structure, transport and magnetic properties, x-ray absorption and specific heat, as well as calculated band structure, of $\mathrm{SmPt_4Ge_{12}}$. $\mathrm{SmPt_4Ge_{12}}$ represents a ternary skutterudite with a platinum–germanium framework, only accessible upon applying high-pressure synthesis. Samarium has been recognized—besides praseodymium—as one of the most interesting cations in filled skutterudites, which leads to a multitude of complex physical phenomena.

One of the most intensively studied compounds is $\mathrm{SmOs_4Sb_{12}}$, which displays a heavy-fermion ground state with $\gamma = 820$–$880\,\mathrm{mJ\,mol^{-1}\,K^{-2}}$ which is remarkably stable in high magnetic fields [25, 26]. In this compound, Sm is not in the Kondo regime but clearly intermediate-valent with $\nu = 2.83$ at 300 K (slightly decreasing with temperature) [27]. In x-ray diffraction (XRD) data the cation shows the largest displacement factor in the $R\mathrm{Os_4Sb_{12}}$ series. This behaviour of the thermal displacement of the cations has been paraphrased as 'rattling' in the literature. In $\mathrm{SmOs_4Sb_{12}}$, it corresponds to a low-lying excitation with a characteristic Einstein temperature Θ_E of only 40(2) K [28, 29]. The 'rattling' f-element has been made responsible for the magnetically robust HF state of $\mathrm{SmOs_4Sb_{12}}$ [30]–[32]. Regarding the crystal electric field (CEF) there are contradicting conclusions from specific heat data: while one group claims that the Sm ions in the $4f^5$ (majority) state have a doublet ground state and an excited quartet state ($\Delta E = k_\mathrm{B} \times 37\,\mathrm{K}$ [25]), another collaboration favours a quartet ground state [26]. Interestingly, also a kind of weak ferromagnetic order is discussed for $\mathrm{SmOs_4Sb_{12}}$ [25].

Connected to the high degeneracy of the quartet ground state in other Sm-filled skutterudites (e.g. $\mathrm{SmFe_4P_{12}}$, a ferromagnetic Kondo lattice [33, 34], $\mathrm{SmRu_4P_{12}}$ showing a metal–insulator transition [34]), multipolar ordering scenarios are under discussion in [35]. The less investigated compounds are $\mathrm{SmFe_4Sb_{12}}$ [36] and $\mathrm{SmFe_4As_{12}}$ [37].

2. Experimental

2.1. Sample preparation

Preparation of the precursor alloys was performed by arc melting of the elements Sm (Dr G Lamprecht, 99.9 wt.%), Pt (ChemPur, 99.9 wt.%) and semiconductor-grade Ge (ChemPur, 99.9999 wt.%). The resulting ingot was sealed in a tantalum ampoule that was encapsulated in an evacuated quartz container. After annealing at 970 K for 7 days the crude product was quenched in water. Sample handling including the prearrangement of the octahedral high-pressure setup was performed in argon-filled glove boxes (MBraun, $p(H_2O) < 1$ ppm; $p(O_2) < 1$ ppm). In order to avoid contamination with oxygen, the high-pressure assembly was transferred to the press directly before synthesis. After the experiment, the setup was immediately removed from the Walker module and transferred into a glove box where the sample was recovered from the crucible.

High-pressure and high-temperature preparation experiments have been performed in an octahedral multi-anvil press. Force redistribution is realized by a Walker module and MgO octahedra with an edge length of 18 mm [38]. Elevated temperatures are realized by resistive heating of graphite tubes. Pressure and temperature calibration is performed in separate calibration experiments by *in situ* monitoring of the resistance changes of bismuth [39, 40] and by heating runs with a thermocouple, respectively. Hexagonal boron nitride proved suitable as a crucible material. By x-ray powder diffraction or energy dispersive x-ray analysis, no evidence was found for a chemical reaction of the containers with the samples. Accordingly, the synthesized products could be separated from the crucibles without difficulty. For the high-pressure syntheses, typical annealing times were 2 h. Quenching to ambient temperature was realized by turning off the heating current before decompression. The resulting samples are dense and stable in air for months.

2.2. Sample characterization

All samples were characterized by powder XRD performed on a HUBER G670 imaging plate Guinier camera equipped with a Ge monochromator by applying CuK$_{\alpha 1}$ radiation ($\lambda = 1.540\,56$ Å). Phase analysis was performed using the WinXPOW program package (STOE WinXPOW, Version 2, STOE and Cie GmbH, Darmstadt). The lattice parameters were refined by least-squares fitting using the positions of about 30 reflections ($2\theta_{\max} = 100^\circ$). Full profile Rietveld refinement was performed on the same powder patterns using the WinCSD program package [41].

$SmPt_4Ge_{12}$ has a silver-metallic luster, and a differential thermal analysis (DTA) shows that the compound decomposes at 1086 K into $PtGe_2$, Ge and $Sm_3Pt_4Ge_6$ [42]. In preparation for the investigation of homogeneity and phase distribution by light- and electron-optical microscopy the samples were polished using a standard procedure. Spectra up to 25 keV were determined by energy dispersive spectroscopy (EDXS) with a microprobe (Philips XS30 and an attached EDAX system Phoenix Si(Li)) on 30 spots. The samples exhibit only the characteristic x-ray emission lines of Sm, Pt and Ge. The intensities of the Sm and Pt L lines as well as the Ge K lines were used for determining the chemical composition. The presence and composition of additional phases such as Ge or $PtGe_2$ were also verified by EDXS measurements (see table 1).

Table 1. Phase composition from EDXS or XRD phase analysis of '$SmPt_4Ge_{12}$' samples annealed at 1070 K at different pressures. The lattice parameters a are for the phase with $LaFe_4P_{12}$ type. The impurity contents (in vol.%) were estimated from XRD pattern and metallographic cuts. *Composition obtained from EDXS analysis.

Pressure	Phase compositions	a/Å
Ambient	$Sm_{2.9(2)}Pt_{3.9(2)}Ge^{*}_{6.2(2)} + Pt_{1.0(2)}Ge^{*}_{2.1(2)} + Ge$	–
4 GPa	$PtGe_2 + Ge + 30\%$ '$SmPt_4Ge_{12}$'	8.610(1)
5 GPa	$Sm_{1.0(1)}Pt_{4.1(1)}Ge^{*}_{11.9(1)} + 2\%\ PtGe_2 + 2\%\ Ge$	8.6069(4)

2.3. *Band structure calculations*

To gain microscopic insight into the electronic structure of $SmPt_4Ge_{12}$, we performed scalar-relativistic and fully relativistic density functional theory (DFT) band structure calculations using the full-potential local-orbital FPLO code (version 9.00-33) [43]. The calculations were performed in the framework of the local density approximation (LDA) by employing the exchange–correlation potential of Perdew and Wang [44]. The first Brillouin zone was sampled by a mesh of $28 \times 28 \times 28$ (21952) k points. The calculations were performed using the experimental structural data. The strongly correlated $4f$ electrons of Sm were treated in the open-core approximation since no convergency could be obtained in $LDA + U$ calculations.

2.4. *Physical properties*

Magnetization at various external fields between 0.02 and 70 kOe was measured by means of a SQUID magnetometer in the temperature range 1.8–400 K (MPMS XL-7, Quantum Design) and from 0.5 to 1.8 K in a field of 1 kOe (^{3}He insert for the MPMS, iQuantum) using a polycrystalline sample ($m \approx 35$ mg). An adjustment of the scale of the ^{3}He susceptibility data by a factor of 1.095 was found to be unavoidable. On the same sample an electrical resistivity measurement was performed with an ac four-point method (0.3–300 K). Due to the geometry of the contacted piece, the inaccuracy of the absolute resistivity is estimated to be ±20%. Specific heat capacity was determined by a relaxation-type method (PPMS, Quantum Design) in the temperature ranges 0.37–10 K and 1.8–320 K.

2.5. *X-ray absorption spectroscopy (XAS)*

The valence state of Sm was investigated by XAS near the Sm L_{III} edge for temperatures down to 5 K. The spectra were recorded in transmission arrangement at EXAFS II beamline A1 of the Hamburg Synchrotron Laboratory (HASYLAB) at DESY. Wavelength selection was realized by means of a Si(111) double crystal monochromator, which yields an energy resolution of approximately 2 eV (FWHM) at the Sm L_{III} threshold of 6716 eV. A helium flow cryostat was used to control the temperature to $\Delta T = 0.1$ K. Experimental data were measured using Sm_2O_3 as an external reference. The average valence of Sm atoms was refined from the obtained spectra using XASWin program [45].

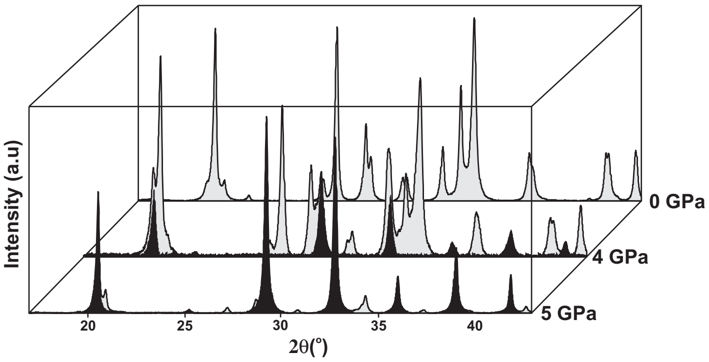

Figure 1. XRD powder patterns (CuK$_{\alpha1}$ radiation) of $SmPt_4Ge_{12}$ synthesis products annealed at 1070 K at different pressures. Reflections belonging to the filled skutterudite-type structure are highlighted in black.

3. Results and discussion

3.1. Crystal structure

RPt_4Ge_{12} compounds with filled-skutterudite crystal structure are known to exist only for $R =$ La–Nd, and Eu [8] (which is divalent in $EuPt_4Ge_{12}$ and therefore of comparable ionic size with the alkaline-earth element Sr). Our attempts to synthesize RPt_4Ge_{12} compounds at ambient pressure with other rare-earth metals failed. Already a sample with formal composition $SmPt_4Ge_{12}$ annealed at 970 K at ambient pressure was found to contain several phases (see table 1) without any trace of cubic skutterudite or related phase. Therefore, we investigated the compound formation under high pressure.

In figure 1, the powder-XRD patterns of a sample with nominal composition $SmPt_4Ge_{12}$ subjected to different pressures at 1070 K are presented. Analysing the XRD data collected for a sample treated at 4 GPa one can already index 12 reflections assuming a cubic body-centred unit cell. This phase with a composition near that of the target phase (as tested by EDXS) is present with a volume fraction of only 30%, indicating that the optimum synthetic conditions are not reached yet. At 5 GPa, the sample is nearly single phase $SmPt_4Ge_{12}$ besides minor amounts of $PtGe_2$ and Ge. The crystal structure of $SmPt_4Ge_{12}$ was (as the major phase, see figure 2) refined assuming isotypism with $LaFe_4P_{12}$ [5] (space group $Im\bar{3}$, $a = 8.6069(4)$ Å, Sm in $2a$ (0, 0, 0); Pt in $8c$ (1/4, 1/4, 1/4); Ge in $24g$ (0, 0.1504(2), 0.3529(2)), $R_I = 0.053$, $R_P = 0.086$). The displacement parameter B_{iso} of Sm is large (1.80(2) Å^2), while those of Pt (0.685(6) Å^2) and Ge (1.01(5) Å^2) are significantly smaller. Interestingly, the filled skutterudite $SmPt_4Ge_{12}$ could not be synthesized at higher pressures. The pressure range for the formation of $SmPt_4Ge_{12}$ is thus rather narrow and the observed differences in the lattice parameters of the filled-skutterudite phases in the 4 and 5 GPa samples could indicate a small phase width, especially with regard to an incomplete filling of the $2a$ site with Sm.

3.2. Electronic band structure

The calculated density of states (DOS) of $SmPt_4Ge_{12}$ is shown in figure 3. Apart from the contribution of the strongly correlated 4f electrons, the calculated DOS, including its partial contributions, is rather similar to that of the superconducting $LaPt_4Ge_{12}$ compound. The DOS

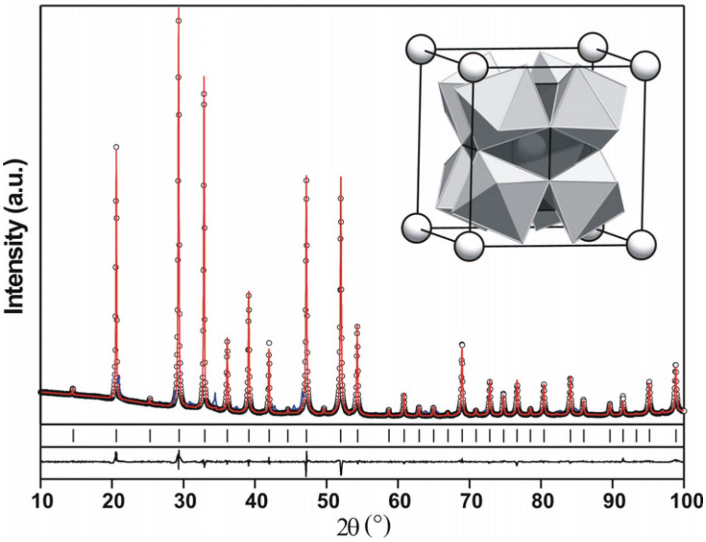

Figure 2. XRD powder data ($CuK_{\alpha1}$ radiation) of the $SmPt_4Ge_{12}$ sample (circles), the refined profile (red line), calculated reflections of the filled skutterudite structure (ticks) and deviations from the calculated profile (black line). The tiny peaks of the $PtGe_2$ excluded from the refinement of the main phase are also shown (blue line). The inset displays the unit cell of the filled skutterudite structure with the $PtGe_6$ octahedra (grey).

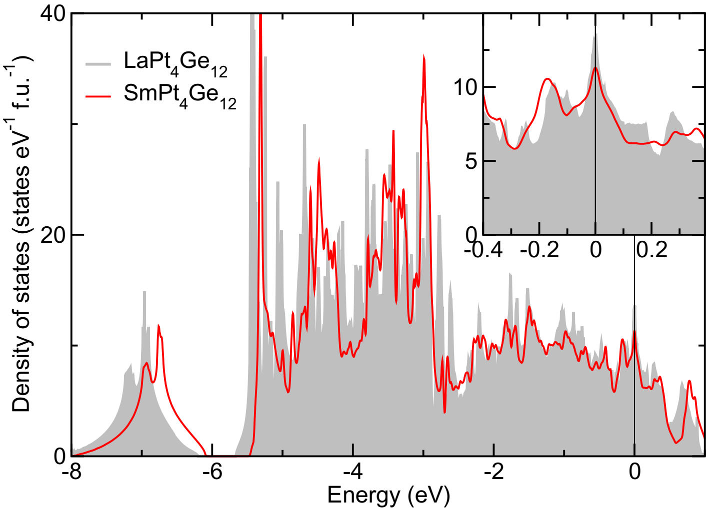

Figure 3. Calculated electronic DOS of $SmPt_4Ge_{12}$ in comparison with that of $LaPt_4Ge_{12}$. The inset shows a magnification around the Fermi level E_F at zero energy.

at the Fermi level E_F is slightly reduced (see the inset in figure 3) compared to $LaPt_4Ge_{12}$ and results in a bare γ_0 value of 26.6 mJ mol^{-1} K^{-2}. This would imply a moderate mass enhancement of ≈3.5 compared to the experimental $\gamma = 92$ mJ mol^{-1} K^{-2} estimated from the specific heat data above 150 K (*vide infra*). However, the role of the correlated 4f electrons

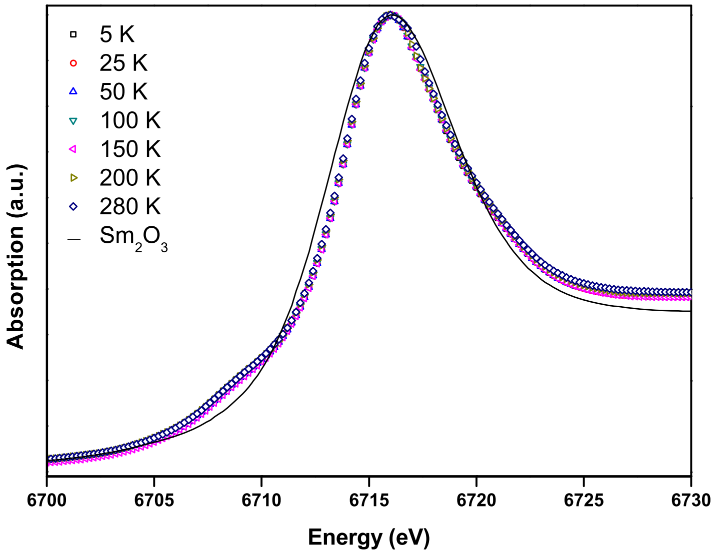

Figure 4. X-ray absorption spectra (XAS) on the Sm L_{III} edge: $SmPt_4Ge_{12}$ at various temperatures (symbols) and Sm_2O_3 at $T = 300$ K (solid line).

and their interaction with the other valence electrons, leading to the observed exotic heavy-fermion behaviour, cannot be discussed within the framework of DFT calculations at present. Including the 4f correlation in a mean-field way applying the LSDA + U approach will lead only to marginal improvement since the dynamic nature of 4f valence fluctuations, responsible for the large linear specific heat coefficient (γ', *vide infra*) below ~10 K, is not taken into account by this method, either. More sophisticated methods such as dynamical mean-field techniques should be applied in future studies to gain deeper insight into the 4f-related many-body physics of $SmPt_4Ge_{12}$.

Some indications for an interaction of f and d orbitals with conduction electrons in $SmPt_4Ge_{12}$ might be already observable in the electron localizability indicator (ELI; [46, 47]) analysis. A structuring of both the fourth shell (due to f orbitals) and the fifth shell (due to d orbitals) of the Sm atom is found. Within the context of an ELI analysis the structuring of an inner atomic shell means an ELI distribution deviating from the spherical one expected for a chemically inert core shell. A structured inner shell implies participation of its electrons in chemical bonding [48, 49]. Details of an ELI analysis of some filled skutterudites will be presented in a forthcoming article [50].

3.3. *Valence of Sm*

A linear dependence of the lattice volume from the ionic radius $V(\mathrm{IR}^{3+})$ for $R =$ La, Ce, Pr and Nd indicates that these ions are trivalent in RPt_4Ge_{12} compounds [50]. On the other hand, Eu in $EuPt_4Ge_{12}$ is stable divalent [8] and the cell volume of $SmPt_4Ge_{12}$ is off the trivalent line $V(\mathrm{IR}^{3+})$. Assuming that the cell volumes of hypothetical divalent RPt_4Ge_{12} compounds lie on a line $V(\mathrm{IR}^{2+})$ parallel to the trivalent one, we can get a first estimate for the average valence $\nu \approx 2.75$ of Sm in $SmPt_4Ge_{12}$. Due to the different compressibilities of di- and trivalent ions the accuracy of this estimate is limited [51].

The XAS of $SmPt_4Ge_{12}$ at ambient temperature measured at the Sm L_{III} edge (figure 4) is dominated by the contribution of the $4f^5$ state (Sm^{3+}), which is clearly seen in the comparison

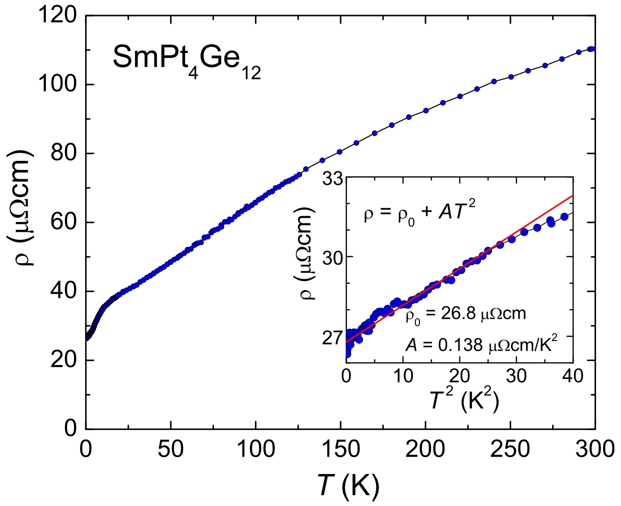

Figure 5. Electrical resistivity ρ versus temperature T of $SmPt_4Ge_{12}$. The inset shows ρ as a function of T^2. The line (red) is a fit according to $\rho(T) = \rho_0 + AT^2$.

with the spectrum of the reference material Sm_2O_3 where Sm is also trivalent. A rather smaller contribution from the $4f^6$ state is visible as a shoulder on the low-energy side of the spectrum. This indicates that Sm atoms are in an intermediate valence state in $SmPt_4Ge_{12}$ with an average valence $\nu = 2.90(3)$. Measurements of several spectra down to a temperature of 5 K demonstrate that the average valence of Sm does not change with temperature within the resolution of the analysis.

3.4. Electrical resistivity

The electrical resistivity of $SmPt_4Ge_{12}$ is given in figure 5. $\rho(T)$ generally increases with temperature but shows a downward curved behaviour from $\approx$10 K to room temperature ($\rho(300\,\mathrm{K}) \approx 100\,\mu\Omega\,\mathrm{cm}$, typical for intermetallic compounds). The residual resistivity ρ_0 of $\approx 27\,\mu\Omega\,\mathrm{cm}$ is high. This is in contrast to polycrystalline $LaPt_4Ge_{12}$ or $PrPt_4Ge_{12}$ samples (synthesized at ambient pressure) with $\rho_0/\rho(300\,\mathrm{K}) = 30$–40 [8]. Below 30 K the behaviour changes and $\rho(T)$ shows a broad shoulder at $\approx$10 K. Such a feature is observed in several Sm-containing skutterudites: in $SmFe_4P_{12}$ at 40 K [24, 33], in $SmFe_4Sb_{12}$ at the ferromagnetic ordering at 43 K [36] and in $SmOs_4Sb_{12}$ around 18 K [25]. Such a behaviour in fact resembles the common (magnetic) Kondo effect. However, in view of the ground-state properties of $SmPt_4Ge_{12}$ (*vide infra*), a much stronger signature of the Kondo effect in the resistivity could be expected. The low-temperature ($T \leqslant 5\,\mathrm{K}$) resistivity follows a $\rho_0 + AT^2$ dependence with $A = 0.138\,\mu\Omega\,\mathrm{cm\,K^{-2}}$ and can thus be described in the framework of a Fermi-liquid picture (see the inset of figure 5).

3.5. Magnetic susceptibility

The magnetic susceptibility is given in figure 6. At high temperatures $1/\chi(T)$ displays the typical Van Vleck behaviour for the $^6H_{5/2}$ ground multiplet and thermal excitations in the $^6H_{7/2}$ excited multiplet of Sm^{3+} [52]. There are deviations from the free ion behaviour, which can

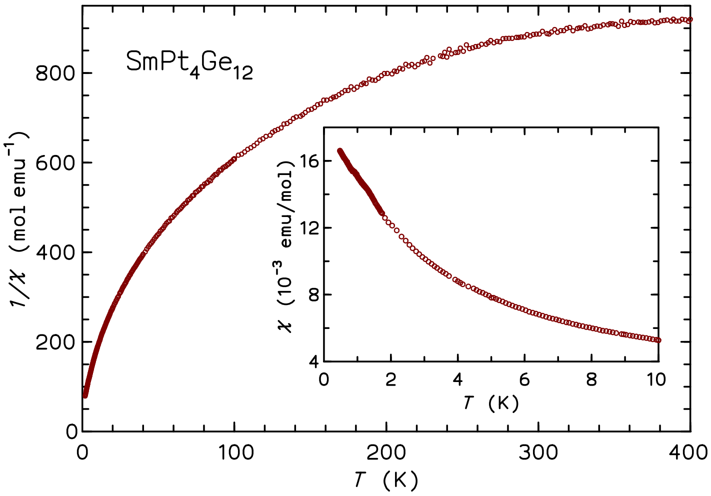

Figure 6. Inverse magnetic susceptibility of SmPt$_4$Ge$_{12}$ for $H = 2$ kOe. The inset shows $\chi(T)$ at low temperature for $H = 1$ kOe. The data taken with the ^{3}He magnetometer have been scaled by a factor of 1.095 to fit the data above 1.8 K.

however not be taken as an indication of a deviation of Sm away from a trivalent valence but can be explained by crystal-field splitting of the ground multiplet. Due to the cubic T_h symmetry of the Sm ion in the filled skutterudite structure the ground multiplet splits into a Γ_{67} quartet (with magnetic and electric degrees of freedom) and a Γ_5 doublet state (only magnetic) [35]. The susceptibility at intermediate temperatures is therefore difficult to interpret. We can draw, however, certain conclusions on the CEF ground state of the ion, especially from specific heat data. The isothermal magnetization $M(H)$ at 1.8 K is very small and $M(H)$ increases only to $0.052\mu_B$ f.u.$^{-1}$ at 70 kOe and does not saturate there. The value is well below the saturation moment expected for the Γ_5 doublet state ($0.238\mu_B$ for the Γ_7 doublet in O_h symmetry [53], which corresponds to Γ_5 in T_h). No hysteresis is seen between increasing and decreasing fields. In addition, no indications for magnetic ordering are visible in low-field ($H = 20$ Oe and $T > 1.8$ K; $H = 1$ kOe and $T > 0.5$ K) susceptibility data.

3.6. Lattice specific heat and crystal electric field (CEF) contribution

The specific heats of SmPt$_4$Ge$_{12}$ and LaPt$_4$Ge$_{12}$ are displayed in figure 7. As discussed in detail in previous publications [8, 54], the specific heat of a (non-magnetic) filled skutterudite is well described by a phonon contribution from the relatively rigid host structure ([Pt$_4$Ge$_{12}$] polyanion) and an Einstein term from the weakly bound guest (the 'rattling' R cation) in the icosahedral site plus a conduction electron Sommerfeld term γT:

$$c_p(T) = c_{\text{host}} + c_{\text{guest}} + \gamma T. \qquad (1)$$

At low temperatures ($T < 10$ K), the host structure contribution may be modelled within the Debye T^3 approximation by a constant initial Debye temperature $\Theta_D(0)$. From a fit to the normal-state specific heat of LaPt$_4$Ge$_{12}$ in the temperature interval 3–10 K (see the inset of figure 7), we obtained $\gamma = 76$ mJ mol^{-1} K^{-2}, $\Theta_D(0) = 209$ K, and an Einstein term with characteristic Einstein temperature $\Theta_E = 96$ K and with the amplitude $3R$ for the full occupancy

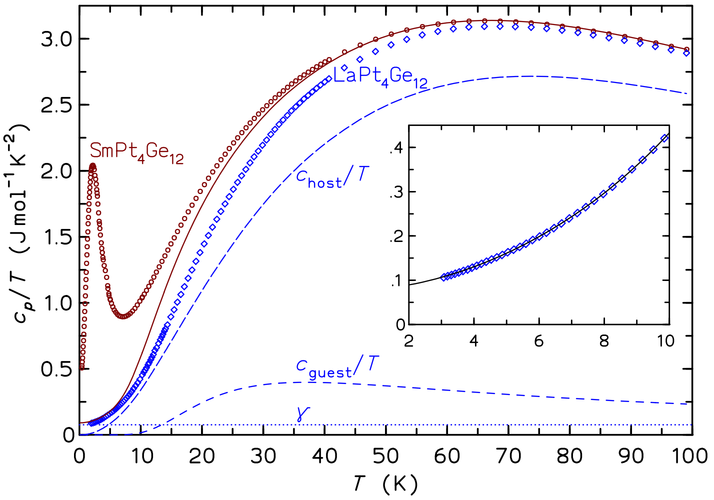

Figure 7. Molar specific heat c_p/T versus temperature T of $SmPt_4Ge_{12}$ (circles, brown) and $LaPt_4Ge_{12}$ (diamonds, blue) [8]. The inset shows the $LaPt_4Ge_{12}$ data used for the fit (diamonds) and the fit curve (see text). The resulting contributions to $c_p(T)$ of $LaPt_4Ge_{12}$ for temperatures up to 100 K are given in the main panel: (i) the host-structure contribution (long-dashed line), (ii) the Einstein contribution of the La guest (short-dashed line) and (iii) the Sommerfeld electronic contribution γT (dotted line). Correcting for the different contributions (ii) and (iii) of $SmPt_4Ge_{12}$ (see text), the non-magnetic contribution $c_p - c_{\mathrm{mag}}$ for $SmPt_4Ge_{12}$ is obtained (full line, brown).

of the guest [8]. The calorimetrically determined value of Θ_{E} is in good agreement with the value calculated from the isotropic displacement parameter B_{iso} of La from XRD data at ambient temperature [50] ($\Theta_{\mathrm{E}}^{\mathrm{IDP}} = 92$ K; for the method and its limitations, especially with respect to incomplete occupancy of the icosahedral site by the cation, see, e.g., [54]–[56]). The calculated temperature dependence of γT and of the Einstein term at higher temperatures are displayed in the main panel of figure 7. The host contribution $c_{\mathrm{host}}(T)$ at higher temperatures is assigned to the difference of the experimental $c_p(T)$ data minus the calculated Einstein and Sommerfeld terms (equation (1)) and is also shown in figure 7.

The host structure contribution to c_p can be assumed to be the same for both compounds. From the displacement parameter $B_{\mathrm{iso}}(300\,\mathrm{K})$ of Sm in $SmPt_4Ge_{12}$, an Einstein temperature $\Theta_{\mathrm{E}} \approx 65$ K is derived that is well below that of $LaPt_4Ge_{12}$. Thus, the total lattice specific heat of the Sm compound at intermediate temperatures is significantly higher than that of the La compound. The sum of the magnetic and electronic contributions for $SmPt_4Ge_{12}$ can now be calculated by using

$$c_{\mathrm{mag}} + c_{\mathrm{e}} = c_p - c_{\mathrm{host}} - c_{\mathrm{guest}} \tag{2}$$

and is plotted in figure 8. At high temperatures it is the sum of a Schottky contribution from CEF excitations and the conduction electron Sommerfeld term γT. The latter term (without possible Kondo-type enhancement) may be determined by examining $c_{\mathrm{mag}} + c_{\mathrm{e}}$ at high T. Above 150 K a linear variation (i.e. $c_{\mathrm{mag}} + c_{\mathrm{e}} \approx \gamma T$) is observed leading to a value $\gamma = 92\,\mathrm{mJ\,mol^{-1}\,K^{-2}}$ that is somewhat higher than that for $LaPt_4Ge_{12}$ (*vide supra*) or $PrPt_4Ge_{12}$ ($87\,\mathrm{mJ\,mol^{-1}\,K^{-2}}$ [8]).

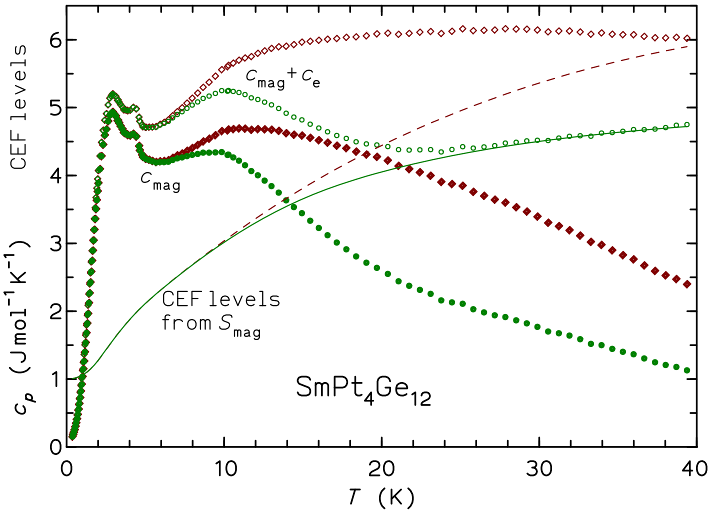

Figure 8. Magnetic and electronic specific heat c_{mag} and c_{e} for SmPt$_4$Ge$_{12}$ (open circles, green), magnetic contribution $c_{\mathrm{mag}}(T)$ (full circles, green) and magnetic entropy $S_{\mathrm{mag}}(T)$ (full line, green) expressed in number of CEF levels. These data have been calculated with Einstein terms with the full amplitude $\epsilon = 3R$. The corresponding higher-lying data (open and full diamonds and dashed line, red) are for the variant with $\epsilon = 19.8\,\mathrm{J\,mol^{-1}\,K^{-1}} < 3R$ (see text).

Using the DOS at the Fermi level E_{F} from the band structure calculations for SmPt$_4$Ge$_{12}$ (11.3 states eV^{-1}, *vide supra*) and taking the enhancement factor as observed for PrPt$_4$Ge$_{12}$ [8], one may calculate $\gamma = 106\,\mathrm{mJ\,mol^{-1}\,K^{-2}}$ for the Sm compound. Interestingly, the enhancement for LaPt$_4$Ge$_{12}$ is significantly weaker. In any case, it is clear that the magnetic and CEF contributions (from the $J = 5/2$ ground multiplet) are only significant below 150 K. However, one scenario we cannot exclude is that the larger-than-expected γ value above 150 K is partially due to CEF excitations from J-mixing, i.e. due to energy levels of the $J = 7/2$ multiplet.

Subtracting the γT term, the consistency of the derived $c_{\mathrm{mag}}(T)$ (figure 8) can be judged from the entropy $S_{\mathrm{mag}}(T)$. For 40 K an entropy of 1.55 R is achieved but not saturated (full line in figure 8). This value suggests that the full entropy $R \ln 6$ expected for the sixfold degenerate ^{6}H$_{5/2}$ ground multiplet of Sm^{3+} is recovered below ~100 K.

In order to check the sensitivity of the procedure against certain changes, the amplitude ϵ of the Einstein mode in LaPt$_4$Ge$_{12}$ was allowed to vary in the fit (see [8]), which resulted in $\epsilon = 19.8\,\mathrm{J\,mol^{-1}\,K^{-1}} < 3R$. Such a reduced spectral weight of the Einstein mode of the cation is in fact realistic, as has been discussed in detail in our recent publications [54, 57, 58]. It usually does not indicate an incomplete occupancy of the cation site. Assuming the same amplitude of the Einstein term for Sm in SmPt$_4$Ge$_{12}$ results in the same γ at high temperatures but different $c_{\mathrm{mag}}(T)$ at intermediate temperatures (see figure 8). The magnetic entropy resulting at 40 K for this variant is 1.77 R, i.e. almost $R \ln 6$ (figure 8, dashed line). Thus, our check demonstrates that the determined $c_{\mathrm{mag}}(T)$ curves are reasonable, but it also shows that the accuracy is insufficient for an exact analysis of the CEF scheme.

As already mentioned, the possible CEF scheme of Sm in a filled skutterudite consists only of a quartet and a doublet (both Kramers states). We tried to model the data in figure 8 with the corresponding Schottky anomalies but could not find a good fit. On the one hand, a

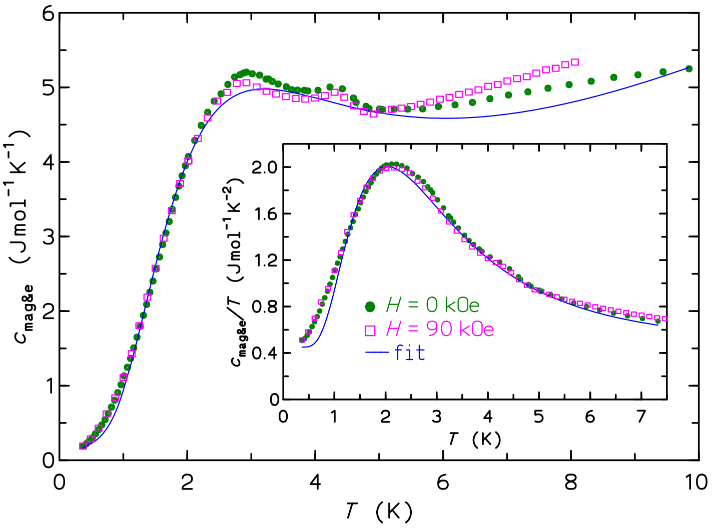

Figure 9. Magnetic–electronic specific heat $c_{\mathrm{mag\&e}}(T)$ for $\mathrm{SmPt_4Ge_{12}}$ in zero field (full circles, green) and in a field of 90 kOe (squares, magenta). The Schottky-type fit described in the text is given as a solid line (blue). The inset shows the same data in a c/T representation.

crystal-field model with a quartet ground-state and excited doublet can reproduce the temperatures of the two broad maxima of $c_p(T)$ but lies significantly below the experimental data in the whole temperature range below 40 K. On the other hand, a model with a doublet ground-state and excited quartet at $\Delta E/k_B = 28$–32 K reproduces the shape of the higher-temperature broad maximum only when scaling it by a factor of 0.7. However, the evolution of S_{mag} with temperature suggests that the features in $c_p(T)$ below 6 K originate from a doublet since the entropy of $R\ln 4$ expected for a quartet ground-state is attained only at $\approx$16 K. Similarly to observations in $\mathrm{SmOs_4Sb_{12}}$ [25], one may assume that a part of the magnetic entropy is absorbed in the correlated state at low temperatures (*vide infra*) at the cost of the crystal field at elevated temperatures. From this entropy argument, we therefore have to conclude that the ground-state is the Γ_5 doublet and the excited quartet Γ_{67} is located at $\Delta E/k_B \approx 30$ K. It has to be mentioned that the non-integral valency of Sm (see the XAS data) is not considered in this argument since it is not obvious from the thermodynamic data.

3.7. Magnetic and electronic specific heat

The magnetic and electronic specific heat $c_{\mathrm{mag\&e}}$ (figure 9) at low temperatures displays a broad maximum around 2.9 K and a small sharp peak at 4.4 K. While looking like a long-range order transition, there is no anomaly detectable in the other measured properties at the temperature of the peak. At 0.369 K (the lowest measured temperature), $(c_{\mathrm{mag}} + c_{\mathrm{e}})/T$ has a value of 500 mJ mol^{-1} K^{-2} and an extrapolation leads to an enhanced Sommerfeld coefficient $\gamma' \approx 400$ mJ mol^{-1} K^{-2}. Regarding the sizable entropy the broad maximum has to be due to the Sm magnetic states.

We tried to fit the data below 10 K with the sum of $\gamma' T$ and a Schottky-type contribution (the phonon correction does not play a role in this temperature range). The resulting parameters are $\gamma' = 450(30)$ mJ mol^{-1} K^{-2} and two energy levels with a degeneracy ratio of 1 : 1 split by

$\Delta E/k_B = 6.6(2)$ K. The very large value of γ' agrees with the previous estimate and qualifies $SmPt_4Ge_{12}$ as a heavy-fermion compound.

In figure 9, also the influence of a magnetic field of 90 kOe on $c_{mag\&e}$ is shown. The specific heat shows no significant changes in field, not even at 0.36 K. Since Sm^{3+} with $J = 5/2$ has only Kramers states, the question of the cause of the splitting of the ground-state and the negligible effect of a magnetic field arises. The latter might be due to a very small g factor of this ground-state doublet of Sm [53]. It is also improbable that the large zero-field splitting of the Kramers doublet is due to magnetic exchange and RKKY interactions. The isostructural compounds $Nd^{3+}Pt_4Ge_{12}$ and $Eu^{2+}Pt_4Ge_{12}$, both with Kramers-degenerate CEF ground-states, show sizable magnetic exchange interactions as judged from the Weiss parameter of the Curie–Weiss fits, $\theta_P = -1.84$ and -17 K, respectively [8, 9]. These interactions lead, however, to an antiferromagnetic ordering at only 0.67 and 1.7 K, respectively [8, 9].

We have no explanation why the low-temperature specific heat can be fitted with the sum of a moderately enhanced γ' and a Schottky-type anomaly. The latter contribution can originate from any kind of two-level system. Thus, the complete non-phononic specific heat $c_{mag\&e}$ has to be regarded as the result of a hybridization of conduction electrons and localized Sm f-states.

The origin of this exotic heavy-fermion ground-state of $SmPt_4Ge_{12}$ is unclear. The usual magnetic Kondo effect seems to be too weak to produce such a large hybridized specific heat. An alternative mechanism for the enhancement of the Sommerfeld parameter was recently suggested by Hotta [30]. Here, the 'rattling' cation in the Sm-filled skutterudite $SmOs_4Sb_{12}$ with a very low-lying Einstein temperature $\Theta_E = 40(2)$ K [28, 29] is made responsible for the hybridization. Moreover, such an HF state should be 'robust' against high magnetic fields, as it is the case for $SmOs_4Sb_{12}$ (see [25, 26, 32]) and in $SmPt_4Ge_{12}$ (higher-field data may be required to corroborate this finding). While the γ' for the Os–Sb system is as high as 820–880 mJ mol^{-1} K^{-2}, only about half the value is attained in $SmPt_4Ge_{12}$. Equally, the characteristic Einstein temperatures of the Sm cation are higher in the Sm-Ge skutterudite.

4. Summary

In conclusion, we have synthesized a new member of the RPt_4Ge_{12} filled skutterudite compounds with $R = Sm$. Samarium is hitherto the smallest rare-earth cation that could be incorporated into the $[Pt_4Ge_{12}]$ host structure. Despite having less spacious icosahedral voids than the iron–pnictogen skutterudites, the void diameter in the $[Pt_4Ge_{12}]$ host structure allows for a large displacement parameter of the Sm ion. Sm in $SmPt_4Ge_{12}$ is in an intermediate but temperature-independent valence state ($\nu = 2.90 \pm 0.03$). Similar to observations in samarium iron-group-metal pnictogen skutterudites, a Kondo-like behaviour is observed in $SmPt_4Ge_{12}$ at low temperatures. A remarkably magnetic-field-independent heavy electron state is observed in specific heat data below $T \approx 10$ K. We conjecture that the origin of this exotic behaviour is very similar to that of the even more pronounced heavy-fermion state in $SmOs_4Sb_{12}$. We propose an approximate crystal-field level scheme of the samarium and the characteristic Einstein temperature of the low-lying Sm-dominated phonon mode ($\Theta_E \approx 65$ K). Whether the intermediate valence of Sm is an ingredient for the formation of the heavy-fermion state is an open question. Comparing $SmPt_4Ge_{12}$ and $SmOs_4Sb_{12}$, we speculate that the relative energy of the Sm Einstein phonon excitation with respect to the Sm crystal-field doublet–quartet excitation determines the strength of the hybridization leading to the exotic heavy-fermion states in both compounds.

Acknowledgments

We thank P Thalmeier and K Gofryk (LANL) for interesting and valuable discussions. We acknowledge the help of F Jach and K Pinkert, who were involved in exploratory syntheses at an early stage. We thank H Borrmann and S Hückmann for performing the XRD experiments and S Leipe and R Koban for assistance.

References

[1] Sales B C, Mandrus D and Williams R K 1996 *Science* **272** 1325–8
[2] Chen G, Dresselhaus M S, Dresselhaus G, Fleurial J and Caillat T 2003 *Int. Mater. Rev.* **48** 45
[3] Uher C 2008 *Chemistry, Physics and Materials Science of Thermoelectric Materials: Beyond Bismuth Telluride* ed M G Kanatzidis, T P Hogan and S D Mahanti (Berlin: Springer) p 121
[4] Sales B C 2007 *Int. J. Appl. Ceram. Technol.* **4** 291–6
[5] Jeitschko W and Braun D 1977 *Acta Crystallogr.* B **33** 3401
[6] Uher C 2001 *Semicond. Semimetals* **69** 139–253
[7] Bauer E *et al* 2007 *Phys. Rev. Lett.* **99** 217001
[8] Gumeniuk R, Schnelle W, Rosner H, Nicklas M, Leithe-Jasper A and Grin Yu 2008 *Phys. Rev. Lett.* **100** 017002
[9] Nicklas M, Gumeniuk R, Schnelle W, Rosner H, Leithe-Jasper A, Steglich F and Grin Yu 2010 *J. Phys.: Conf. Ser.* accepted (arXiv:1007.3844)
[10] Toda M, Sugawara H, Magishi K I, Saito T, Koyama K, Aoki Y and Sato H 2008 *J. Phys. Soc. Japan* **77** 124702
[11] Baenitz M *et al* 2010 *Phys. Status Solidi* b **247** 740–2
[12] Kaczorowski D and Tran V H 2008 *Phys. Rev.* B **77** 180504
[13] Bauer E, Chen X, Rogl P, Hilscher G, Michor H, Royanian E, Podloucky R, Giester G, Sologub O and Gonçalves A P 2008 *Phys. Rev.* B **78** 064516
[14] Sekine C, Uchiumi T, Shirotani I, Matsuhira K, Sakakibara T, Goto T and Yagi T 2000 *Phys. Rev.* B **62** 11581
[15] Shirotani I, Shimaya Y, Kihou K, Sekine C and Yagi T 2003 *J. Solid State Chem.* **174** 32–4
[16] Shirotani I 2003 *Bull. Chem. Soc. Japan* **76** 1291–307
[17] Shirotani I, Araseki N, Shimaya Y, Nakata R, Kihou K, Sekine C and Yagi T 2005 *J. Phys.: Condens. Matter* **17** 4383–91
[18] Kihou K, Shirotani I, Shimaya Y, Sekine C and Yagi T 2004 *Mater. Res. Bull.* **39** 317–25
[19] Yamanaka S, Enishi E, Fukuoka H and Yasukawa M 2000 *Inorg. Chem.* **39** 56–8
[20] Schwarz U, Wosylus A, Böhme B, Baitinger M, Hanfland M and Grin Yu 2008 *Angew. Chem., Int. Ed. Engl.* **47** 6790–3
[21] Wosylus A, Prots Y, Burkhardt U, Schnelle W, Schwarz U and Grin Yu 2006 *Solid State Sci.* **8** 773–81
[22] Wosylus A, Veremchuk I, Schnelle W, Baitinger M, Schwarz U and Grin Yu 2009 *Chem. Eur. J.* **25** 5901–3
[23] Sales B C 2003 *Handbook on the Physics and Chemistry of Rare Earths* vol 33, ed K A Gschneidner, J-C G Bünzli and V K Pecharsky (Amsterdam: Elsevier) chapter 211, pp 1–34
[24] Sato H, Sugawara H, Aoki Y and Harima H 2009 *Handbook of Magnetic Materials* vol 18, ed K H J Buschow (Amsterdam: Elsevier) pp 1–110
[25] Yuhasz W M *et al* 2005 *Phys. Rev.* B **71** 104402
[26] Sanada S, Aoki Y, Tsuchiya A, Kikuchi D, Sugawara H and Sato H 2005 *J. Phys. Soc. Japan* **74** 246–9
[27] Mizumaki M, Tsutsui S, Tanida H, Uruga T, Kikuchi D, Sugawara H and Sato H 2007 *J. Phys. Soc. Japan* **76** 053706
[28] Tsubota M, Tsutsui S, Kikuchi D, Sugawara H, Sato H and Murakami Y 2008 *J. Phys. Soc. Japan* **77** 073601
[29] Tsutsui S, Mizumaki M, Tsubota M, Tanida H, Uruga T, Murakami Y, Kikuchi D, Sugawara H and Sato H 2009 *J. Phys.: Conf. Ser.* **150** 042220

[30] Hotta T 2008 *J. Phys. Soc. Japan* **77** 103711

[31] Hotta T 2009 *J. Phys. Soc. Japan* **78** 073707

[32] Sato H 2009 *J. Phys. Soc. Japan Online* News and comments (10 July 2009)

[33] Takeda N and Ishikawa M 2003 *J. Phys.: Condens. Matter* **15** L229–33

[34] Matsuhira K, Doi Y, Wakeshima M, Hinatsu Y, Amitsuka H, Shimaya Y, Giri R, Sekine C and Shirotani I 2005 *J. Phys. Soc. Japan* **74** 1030–5

[35] Kuramoto Y, Kusunose H and Kiss A 2009 *J. Phys. Soc. Japan* **78** 072001

[36] Ueda M, Kawahito Y, Tanaka K, Kikuchi D, Aoki H, Sugawara H, Kuwahara K, Aoki Y and Sato H 2008 *Physica* B **403** 881–3

[37] Kikuchi D, Tatsuoka S, Tanaka K, Kawahito Y, Ueda M, Shinozawa A, Aoki H, Kuwahara K, Aoki Y and Sato H 2008 *Physica* B **403** 884–6

[38] Walker D, Carpenter M A and Hitch C M 1990 *Am. Mineral.* **75** 1020–8

[39] Young D A 1991 *Phase Diagrams of the Elements* (Berkeley, CA: University of California Press)

[40] Walter M J, Thibault Y, Wei K and Luth R W 1995 *Can. J. Phys.* **73** 273–86

[41] Akselrud L G, Zavalii P Y, Grin Yu, Pecharsky V K, Baumgartner B and Wölfel E 1993 *Mater. Sci. Forum* **133–136** 335

[42] Imre A, Hellmann A and Mewis A 2006 *Z. Anorg. Allg. Chem.* **632** 1145–9

[43] Koepernik K and Eschrig H 1999 *Phys. Rev.* B **59** 1743

[44] Perdew J P and Wang Y 1992 *Phys. Rev.* B **45** 13244

[45] Akselrud L G and Grin Yu 2004 *XasWin Program* Max-Planck-Institut für Chemische Physik fester Stoffe, Dresden

[46] Kohout M 2004 *Int. J. Quantum Chem.* **97** 651

[47] Kohout M 2007 *J. Chem. Soc. Faraday Trans.* **135** 43

[48] Kohout M, Wagner F R and Grin Yu 2002 *Theor. Chem. Acc.* **108** 150

[49] Wagner F R, Bezugly V, Kohout M and Grin Yu 2007 *Chem. Eur. J.* **13** 5724

[50] Gumeniuk R, Borrmann H, Ormeci A, Schnelle W, Nicklas M, Rosner H, Leithe-Jasper A and Grin Yu 2010 *Z. Kristallogr.* accepted

[51] Neumann G, Pott R, Röhler J, Schlabitz W, Wohlleben D and Zahel H 1982 *Valence Instabilities* ed P Wachter and H Boppart (Amsterdam: North Holland) pp 87–91

[52] Lueken H 1999 *Magnetochemie* (Stuttgart, Leipzig: B G Teubner)

[53] Buschow K H J, van Diepen A M and de Wijn H W 1973 *Phys. Rev.* B **8** 5134–8

[54] Schnelle W, Leithe-Jasper A, Rosner H, Cardoso-Gil R, Gumeniuk R, Trots D, Mydosh J A and Grin Yu 2008 *Phys. Rev.* B **77** 094421

[55] Sales B C, Chakoumakos B C, Mandrus D, Sharp J W, Dilley N R and Maple M B 1998 *Thermoelectric Materials 1998—The Next Generation Materials for Small Scale Refrigeration and Power Generation Applications* ed T M Tritt, M G Kanatzidis, G D Mahan and H B Jr Lyon vol 545 (Warrendale, PA: Materials Research Society) p 13

[56] Sales B C, Mandrus D and Chakoumakos B C 2001 *Semicond. Semimet.* **70** 1–36

[57] Leithe-Jasper A, Schnelle W, Rosner H, Cardoso-Gil R, Baenitz M, Mydosh J A, Grin Yu, Reissner M and Steiner W 2008 *Phys. Rev.* B **77** 0644212

[58] Koza M M, Capogna L, Leithe-Jasper A, Rosner H, Schnelle W, Mutka H, Johnson M R, Ritter C and Grin Yu 2010 *Phys. Rev.* B **81** 174302